Proceedings of
International Conference on Science and Sustainable Development (ICSSD)
"The Role of Science in Novel Research and Advances in Technology"
Center for Research, Innovation and Discovery, Covenant University, Nigeria
June 20-22, 2017

Research Article

The Prospect of Micro-Energy Generation from Almond (Prunus Dulcis) Dye-Sensitized Solar Cells

T.J. Abodunrin[1], A.O. Boyo[2], M.R. Usikalu[1,*], L. Obafemi[1] and F. Oladapo[1]

[1] *Department of Physics, Covenant University, Ota, Ogun State, Nigeria*
[2] *Department of Physics, Lagos State University, Ojo, Badagry Express, Nigeria*
***Corresponding author:** mojisola.usikalu@covenantuniversity.edu.ng*

Abstract. The generation of environmentally and sustainable energy is a basic need towards proffering a solution to the climatic and scientific challenges confronting twenty-first century human race. This quest has led to the discovery of diverse unconventional energy resources existing presently. Amongst all these viable options, solar energy is considered to have the best prospect in view of its all-year availability, no geographical restriction and the 3.8×10^{26} Joule of energy it gives off per second. This energy can be tapped either using direct or indirect means; the use of natural dyes to mimic photosynthesis in *dye-sensitized solar cell* (DSC) device is a response to provide an economical and technical substitute to traditional *p-n* junction photovoltaic devices. DSC is a systematic device that uses disorderly technology to produce electricity in diverse light conditions such as outdoors, in poor lightning conditions. The devices are also able to convert both natural and man-made light into energy to power technology through a broad range of electronic devices. In this paper, we present almond dye-sensitized cells spectral responses with four different electrolyte sensitizers. The result is DSCs with a comparative output efficiency of 3.24%, Voc of 306 mV with KBr; the least efficient DSC was $HgCl_2$ electrolyte sensitized with an output efficiency of 0.09% under same standard atmospheric conditions of 1.5 A.M and temperature of $27.1\,^{\circ}$C and pH of 5.49.

Keywords. Micro-energy generation; Dye-sensitized solar cell; Spectral responses; Almond; Sustainable energy

MSC. 92C80

1. Introduction

The word "almond" originates from ancient French almande or alemande. The almond (Prunus dulcis) is a class of tree native to India, Middle East, and North Africa. "Almond" is also the name of the appetizing and extensively grown seed of this tree. Amongst the Prunus species, it is grouped as peach in the subgenus Amygdalus. The almond fruit is a drupe; the leaves are 3-5 inches long (Figure 1), with a serrated margin and a 2.5 cm petiole [3].

At a time when the adverse consequences of past and present fossil fuel consumption is creating havoc in world climatic pattern and decimating fossil reservoir with a looming threat of depletion despite man's huge dependence on its availability; it is imperative to seek sustainable energy types which will be readily available, cheap, easy to manufacture and not be toxic to the environment. Dye-sensitized solar cells possess all these attributes in one device. This therefore makes it a very attractive replacement for fossil fuel indirectly and a direct substitute for conventional silicon solar cells [4]. Dye solar cells (DSCs) are classified by their structural application as thin film cells. The name has its origin in the inventor Grätzel who has played a key role in the advancement of novel types of solar cells [9]. DSCs known functionally as Photovoltaic devices are based on the concept of charge separation at the boundary interface of two different materials and dissimilar apparatus for conduction [2]. The high efficiency of silicon has led to its predominance in the solar cell technology. However, this control by inorganic solid-state junction devices is presently being sorely tried by each progress and development of third generation solar cells, of which DSCs are examples [11]. The DSC technology makes it possible to leave the prototypical orthodox solid-state junction device, by replacing the *p-n* junction and limiting factors with a single mechanism which is able to combine the dual process of charge separation and transport in a single mechanism efficiently [1]. The remarkable advances recorded in the synthesis, build up and characterization of solar cells has unlocked enormous possibilities for subsequent applications for these systems. The study of the quantity of dye adsorbed unto the photoanode framework can be carried out by altering the form and structure of the semiconductor [15]. The properties of the dye solution influence the volume of dye adsorbed unto the photoanode frame [7]. A factor responsible for determining the concentration of the solution is the choice of electrolyte sensitizer [8].

Although the efficiency of organic photovoltaics such as DSCs is still less than traditional silicon solar cells, the gap is being reduced steadily by investigations into the factors affecting optical absorption and the charge separation processes by introducing different redox mediators of sensitizer as contacting phase to the semiconductor.


Figure 1. Almond fruit leaf (*P.dulcis*)

2. Materials and Method

4.0 Kg of *P.dulcis* leaves was harvested and air dried until it assumed a constant mass. It was milled and soaked in 500 l of methanol for several days to extract the dye. This liquor mixture was placed in a Stuart RE300 B rotary evaporator, to recover the dye from its mother liquor [14]. The pH and temperature of *P.dulcis* leaf extract were determined by a handheld pH meter. 1 g of the extract was dissolved in 100 g of distilled water (DW) to determine the phytoconstituents. Again 1 g of *P.dulcis* extract was dissolved in methanol to obtain the UV/Vis measurements using the Thermo-scientific Evolution 60 series UV/Vis spectrophotometer. The same ratio of extract was used to determine the FTIR measurement using the Shimadzu FTIR spectrophotometer.

The doctor blade method was used to apply 1g of *P.dulcis* dye onto ITO glass (75 mm × 25 mm) and surface resistivity 10 ohm/m^2. Vecstar furnaces were used for high temperature sintering to 450 °C of the titanium oxide photoanode. An active area of 15.17 cm^2 was exposed to radiation.

A Voltcraft M-3850 series digital multimeter was connected in parallel with a variable resistor to obtain the photoelectric values of *P.dulcis* DSCs.
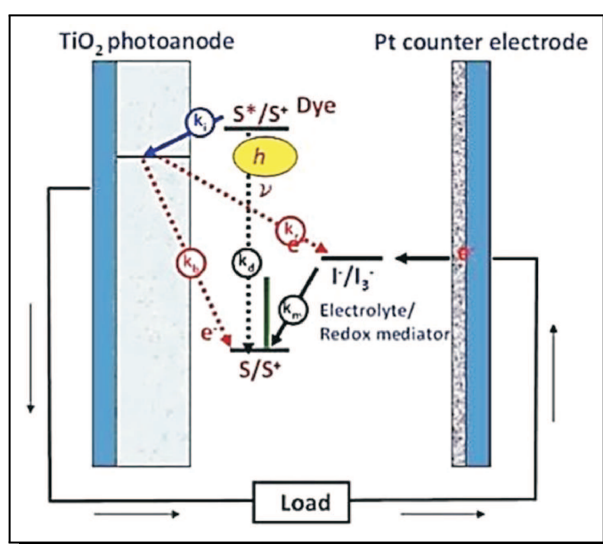
Figure 2. Schematic Diagram and working operation of a dye-sensitized solar cell

This occurs in various avenues such as by a liquid electrolyte, sol gel or solid, thus establishing it as an operational photo-electrochemical cell. The working operation of a DSC is described by the following steps: When incident light of appropriate frequency strikes the solar cell, it disrupts its quantum state by liberating excited electrons from the surface of a photosensitive monolayer of dye as shown in Figure 2 [13]. The dye can be natural or synthetic; its role is mimicry of chlorophyll in photosynthesis. The dye also provides a medium for emission of the electrons into the titanium framework. This creates an ambience for electron transport as electrolyte solutions is introduced in the interface between the dye and photoanode structure [12]. Thus the electrolyte conducts the charges to a back contact to complete the circuitous route; the load represents the work done by the energy produced. This electrolyte engages in a

reversible reaction of continuous reduction and oxidation of the dye as the ion exchange occurs. It is self-sustaining and ought to be capable of lasting twenty years of outdoor applications [6]. In this work, the performance of *P.dulcis* dye-sensitized solar cells analyzed with four different sensitizers at same concentrations was studied. The effect of pH, optimal temperature on the performance of the cells was also reported.

3. Results and Discussion

3.1 Phytochemical Screening

The chromophores present in *P.dulcis* are reported in Table 1. These represent the vehicle for the electron transport to the titanium framework. The result shows tannins, saponins, cardiac glycosides and phenols being highly present. This suggests a higher preference for the preferential choice of any of these chromophores except where the kinematics of the reaction favors other compounds. Flavonoids and alkaloids are available in traces in *P.dulcis* extract; they may be used for charge transport but not preferentially. It would be only due to favorable chemical kinematics [5].

Table 1. Qualitative phytochemical constituent of *P.Dulcis* leaf

|	Constituent	Appearance
1	Carbohydrate (CHO)	−
2	Tannin	++
3	Saponin	++
4	Flavonoid	+
5	Alkaloid	+
6	Quinone	−
7	Glycoside	−
8	Cardiac Glycoside	++
9	Terpenoid	−
10	Phenol	++
11	Steroid	−

3.2 UV/Vis Spectroscopy

The UV/Vis spectrograph in Figure 3 illustrated a maximum absorbance within the visible region ($\lambda_{\max}$). This affirms that *P.dulcis* is a colored substance and absorbs most at a wavelength of 661 nm. The implication of this is that, it absorbs red light and appears to be blue-green in colour. When light impinges on *P.dulcis*, its valence electrons are excited from their ground state to excited states. The

$$v = f\lambda \tag{1}$$

Where V: velocity of light (3×108 m/s); λ: wavelength of absorption.

The frequency is thus given by

$$\frac{V}{\lambda} = 4.5 \times 1014 \text{ Hz} \tag{2}$$
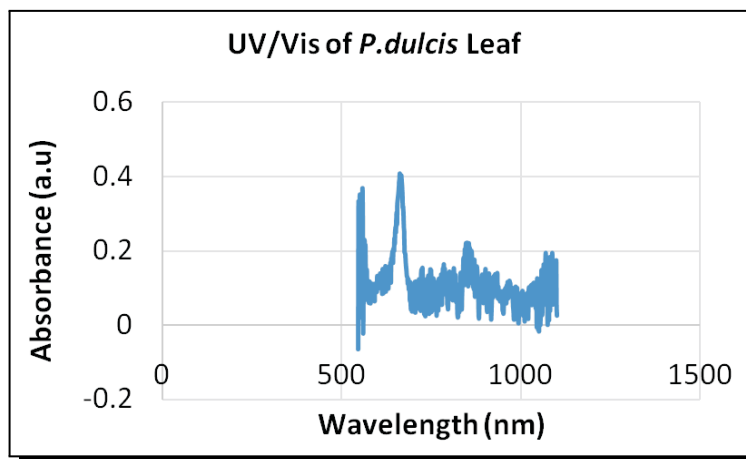
Figure 3. UV/Vis of *P.dulcis* leaf

A high frequency is proportional to a large energy transmission which will promote π to π^*, n to σ^* and n to π^* electronic transitions.

In accordance with Beer-Lambert's law:

$$A = \varepsilon cl \tag{3}$$

Where A : Absorbance;

ε: Molar absorbance coefficient ($\text{mol}^{-1}\ \text{dm}^3$);

c: Concentration (mol dm^{-3});

l: Path length (cm)

The values of ε and $\lambda_{\max}$ are intensely affected by conjugation and degree of substitution [10].

3.3 FTIR Spectroscopy

The fingerprint of *P.dulcis* at $441\,\text{cm}^{-1}$ belongs to a skeletal vibration of chlorite mineral in Si–O–Mg deformation. 555.52 to $719.47\,\text{cm}^{-1}$ features any type of chloroalkane (C–X bond) from weak to medium appearance. Wavelength of $877.64\,\text{cm}^{-1}$; depicts aromatic C–H bond of meta-disubstituted benzene presenting a strong appearance. C–X bonds feature again between $1000\text{-}1200\,\text{cm}^{-1}$ wavelength as ordinary and trifluromethyl types of bond presenting as two strong broad bands. At $1234.48\,\text{cm}^{-1}$ strong phosphate bonds appear. From 1323 to $1460\,\text{cm}^{-1}$, very strong S=O bonds present as sulfone, sulfonic acid, sulfonyl chloride and sulfate respectively. Peak range of $1,615\text{-}1700\,\text{cm}^{-1}$ represent any type of C=N bond with similar conjugation effects as C=O. Specific peak $1735.99\,\text{cm}^{-1}$ corresponds to carboxylic acids and derivatives in esters and lactones which are influenced by ring size and conjugation. Wavelength $2046.47\,\text{cm}^{-1}$ is the presence of any C=N bond of R-N=C=S type. The range 2400 to $3200\,\text{cm}^{-1}$ shows any multiple broad peaks of ammonium ions. Finally, wavelength $3423.73\,\text{cm}^{-1}$ represents any strong primary amine in N-H type of bond (Figure 4) [10].

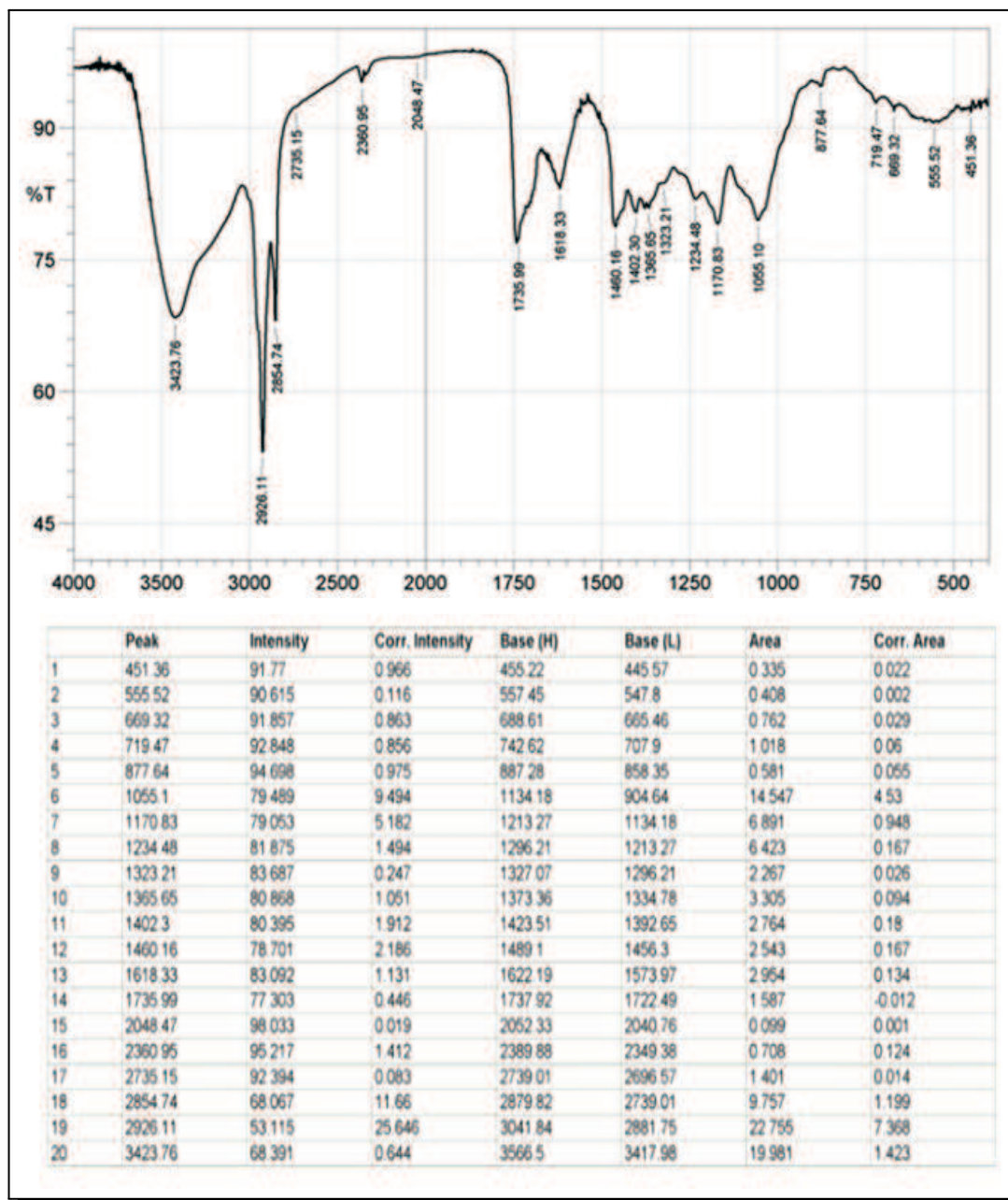|	Peak	Intensity	Corr. Intensity	Base (H)	Base (L)	Area	Corr. Area
1	451.36	91.77	0.966	455.22	445.57	0.335	0.022
2	555.52	90.615	0.116	557.45	547.8	0.408	0.002
3	669.32	91.857	0.863	688.61	665.46	0.762	0.029
4	719.47	92.848	0.856	742.62	707.9	1.018	0.06
5	877.64	94.698	0.975	887.28	858.35	0.581	0.055
6	1055.1	79.489	9.494	1134.18	904.64	14.547	4.53
7	1170.83	79.053	5.182	1213.27	1134.18	6.891	0.948
8	1234.48	81.875	1.494	1296.21	1213.27	6.423	0.167
9	1323.21	83.687	0.247	1327.07	1296.21	2.267	0.026
10	1365.65	80.868	1.051	1373.36	1334.78	3.305	0.094
11	1402.3	80.395	1.912	1423.51	1392.65	2.764	0.18
12	1460.16	78.701	2.186	1489.1	1456.3	2.543	0.167
13	1618.33	83.092	1.131	1622.19	1573.97	2.954	0.134
14	1735.99	77.303	0.446	1737.92	1722.49	1.587	-0.012
15	2048.47	98.033	0.019	2052.33	2040.76	0.099	0.001
16	2360.95	95.217	1.412	2389.88	2349.38	0.708	0.124
17	2735.15	92.394	0.083	2739.01	2696.57	1.401	0.014
18	2854.74	68.067	11.66	2879.82	2739.01	9.757	1.199
19	2926.11	53.115	25.646	3041.84	2881.75	22.755	7.368
20	3423.76	68.391	0.644	3566.5	3417.98	19.981	1.423

Figure 4. FTIR of *P.dulcis* leaf extract

3.4 Photoelectric Parameters

The result of the I-V characteristic curve (Figure 5) for *P.dulcis* is summarized on Table 2.

The most efficient *P.dulcis* DSC is that sensitized with KBr electrolyte, it has an output efficiency of 3.24%; this is due to the quality of the cell as shown by the fill factor. This suggests good interboundary interface between the photoanode/electrolyte/*P.dulcis* dye. The least efficient DSC is that sensitized with HgCl2 because of poor interfacial contact at the boundary interface of the photoanode/electrolyte/*P.dulcis* dye. The work done in the circuit by electron transport is highest for KI electrolyte; Voc has the highest value (306 mV).
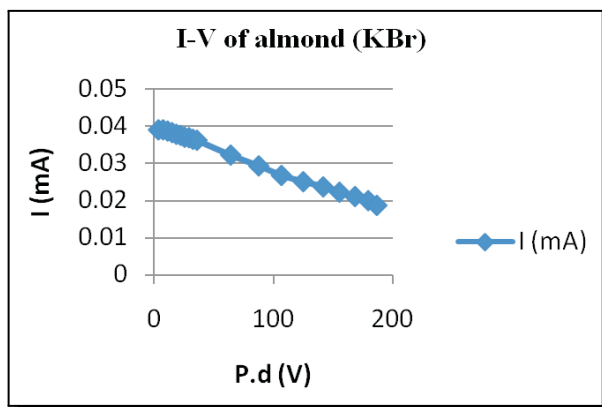
Figure 5. I-V of *P.dulcis* leaf DSC

Table 2. Photoelectric values of *P.Dulcis* DSCs

	HgCl2	KI	KBr	KCl
Isc (mA)	0.019	0.245	0.039	0.068
Voc (mV)	175.50	306.00	186.80	19.10
Pmax(W)	1.19	19.10	1.19	0.05
ff	2.80	0.39	6.12	2.59
η	0.09	0.29	3.24	0.34

[a]: The Phytoconstituents of *P.Dulcis* leaf extract
[b]: The Photoelectric parameters of *P.Dulcis* DSCs with different electrolytes

This implies few recombination occurred due to a small number of trap sites. KCl records the least Voc probably because of a high dark current. The fill factor suggests a good quality DSC devoid of trap sites.

The same electrolyte concentration of 1 part electrolyte solute: 100 ml DW was used. However, different spectral responses were evoked as illustrated on Table 2. The temperature of *P.dulcis* extract was recorded as $27.1\,^{\circ}$C. A pH of 5.49 indicates the reaction kinetics happened within the acidic medium. This collaborates with the FTIR result in strong sulfonic acids presenting and the carboxylic acid conjugation. This further suggests a preferential discharge of these ions as they engage in charge transport. This indicates that the phenol phytoconstituents was actively used in the electron transport.

4. Conclusion and Recommendation

The efficiency output of KBr electrolyte sensitized *P.dulcis* DSC encourages mass production in modules. This is because the kinematics of the reaction is positive and the interfacial boundary contact is favorable for the optimal temperature and pH conditions recorded. This suggests that the problem of acid corrosion will be minimized since the reaction promotes the acidic mode naturally.

Acknowledgments

Competing Interests

The authors declare that they have no competing interests.

Authors' Contributions

All the authors contributed significantly in writing this article. The authors read and approved the final manuscript.

References

[1] S.A.M. Al-Bat'hi, I. Alaei and I. Sopyan, Natural photosensitizers for dye sensitized solar cells, *International Journal of Renewable Energy Research* **3** (1) (2013), 138–143.

[2] G. Boschloo and A. Hagfeldt, Characteristics of the iodide/triiodide redox mediator in dye-sensitized solar cells, *Accounts of Chemical Research* **42** (11) (2009), 1819–1826.

[3] M. Grätzel, Recent advances in sensitized mesoscopic solar cells, *Accounts of Chemical Research* **42** (11) (2009), 1788–1798.

[4] S. Hwang, J.H. Lee, C. Park, H. Lee, C. Kim, C. Park, M.H. Lee, W. Lee, J. Park, K. Kim, N.G. Park and C. Kim, A highly efficient organic sensitizer for dye-sensitized solar cells, *Chemical Communications* **46** (2007), 4887–4889.

[5] N.C. Jeong et al., Effective panchromatic sensitization of electrochemical solar cells: strategy and organizational rules for spatial separation of complementary light harvesters on high-area photo electrodes, *J. Am. Chem. Soc.* **134** (2012), 19820–19827.

[6] D. Kuang et al., Co-sensitization of organic dyes for efficient ionic liquid electrolyte-based dye-sensitized solar cells, *Langmuir* **23** (2007), 10906–10909.

[7] S.M. Milenković, J.B. Zvezdanović, T.D. Andjelković and D.Z. Marković, The identification of chlorophyll and its derivatives in the pigment mixtures: HPLC-chromatography, visible and mass spectroscopy studies, *Adv. Tech.* **1** (1) (2012), 16–24.

[8] M.K. Nazeeruddin, A. Kay, I. Rodicio, R. Humpbry-Baker, E. Miiller, P. Liska, N. Vlachopoulos and M. Grätzel, Conversion of light to electricity by cis-X2bis(2,2'-bipyridyl-4,4'-dicarboxylate) ruthenium(II) charge-transfer sensitizers (X = Cl−, Br-, I−, CN−, and SCN−) on nanocrystalline titanium dioxide electrodes, *J. Am. Chem. Soc.* **115** (1993), 6382–6390.

[9] M.K. Nazeeruddin, P. Péchy, T. Renouard, S.M. Zakeeruddin, R. Humphry-Baker, P. Comte, P. Liska, L. Cevey, E. Costa, V. Shklover, L. Spiccia, G.B. Deacon, C.A. Bignozzi and M. Grätzel, Engineering of efficient panchromatic sensitizers for nanocrystalline TiO_2-based solar cells, *Journal of the American Chemical Society* **123** (8) (2001), 1613–1624.

[10] B.C. O'Regan and F. Lenzmann, Charge transport and recombination in a nanoscale interpenetrating network of n-type semiconductors: transient photocurrent and photovoltage studies of TiO_2/dye/CuSCN photovoltaic cells, *J. Phys. Chem. B* **108** (2004), 4342–4350.

[11] S. Sharma, S. Bulkesh, S.K. Ghoshal and D. Mohan, Dye sensitized solar cells: From genesis to recent drifts, *Renewable and Sustainable Energy Reviews* **70** (2017), 529–537.

[12] S. Tontapha, W. Sangaroon, S. Kanokmedhakul, T. Promgool and V. Amornkitbamrung, Effects of dye-adsorption solvents, acidification and dye combination on efficiency of DSSCs sensitized by α-mangostin and anthocyanin from mangosteen pericarp, *J. Mater. Sci.: Mater Electron* (2017).

[13] V. Varadharajan, U.K. Janarthanan and V. Krishnamurthy, Physicochemical, phytochemical screening and Profiling of secondary metabolites of Annona Squamosa leaf extract, *J. Pharmacogn and Phytochem.* **5** (2) (2016), 200–203.

[14] J.H. Yum, E. Baranoff, S. Wenger, M.K. Nazeeruddin and M. Gratzel, Panchromatic engineering for dye-sensitized solar cells, *Energy Environ. Sci.* **4** (2011), 842–857.

[15] Q. Zhang and G. Cao, Nanostructured photoelectrodes for dye-sensitized solar cells, *Nano Today* **6** (1) (2011), 91–109.